THE JOURNAL OF BIOLOGICAL CHEMISTRY VOL. 287, NO. 20, pp. 16230–16237, May 11, 2012
Published in the U.S.A.

Conjugated Fatty Acid Synthesis

RESIDUES 111 AND 115 INFLUENCE PRODUCT PARTITIONING OF MOMORDICA CHARANTIA CONJUGASE[*] [S]

Received for publication, November 17, 2011, and in revised form, March 9, 2012 Published, JBC Papers in Press, March 26, 2012, DOI 10.1074/jbc.M111.325316

Richa Rawat[‡], Xiao-Hong Yu[‡], Marie Sweet[§], and John Shanklin[‡§1]

From the [‡]Department of Biochemistry and Cell Biology, Stony Brook University, Stony Brook, New York 11794 and the [§]Department of Biology, Brookhaven National Laboratory, Upton, New York 11973

Background: *Momordica* conjugase produces α-eleostearic acid, whereas *Punica* or *Trichosanthes* conjugases produce punicic acid.
Results: *Momordica* conjugase residues 111 and 115 affect total eleostearic acid accumulation levels in transgenic *Arabidopsis*.
Conclusion: Interactions of *Momordica* side chains 111 and 115 influence α-eleostearic acid *versus* punicic acid formation.
Significance: *Momordica* conjugase mutant accumulated punicic acid in addition to α-eleostearic acid.

Conjugated linolenic acids (CLNs), 18:3 $\Delta^{9,11,13}$, lack the methylene groups found between the double bonds of linolenic acid (18:3 $\Delta^{9,12,15}$). CLNs are produced by conjugase enzymes that are homologs of the oleate desaturases FAD2. The goal of this study was to map the domain(s) within the *Momordica charantia* conjugase (FADX) responsible for CLN formation. To achieve this, a series of *Momordica* FADX-*Arabidopsis* FAD2 chimeras were expressed in the *Arabidopsis fad3fae1* mutant, and the transformed seeds were analyzed for the accumulation of CLN. These experiments identified helix 2 and the first histidine box as a determinant of conjugase product partitioning into punicic acid (18:3 $\Delta^{9cis,11trans,13cis}$) or α-eleostearic acid (18:3 $\Delta^{9cis,11trans,13trans}$). This was confirmed by analysis of a FADX mutant containing six substitutions in which the sequence of helix 2 and first histidine box was converted to that of FAD2. Each of the six FAD2 substitutions was individually converted back to the FADX equivalent identifying residues 111 and 115, adjacent to the first histidine box, as key determinants of conjugase product partitioning. Additionally, expression of FADX G111V and FADX G111V/D115E resulted in an approximate doubling of eleostearic acid accumulation to 20.4% and 21.2%, respectively, compared with 9.9% upon expression of the native *Momordica* FADX. Like the *Momordica* conjugase, FADX G111V and FADX D115E produced predominantly α-eleostearic acid and little punicic acid, but the FADX G111V/D115E double mutant produced approximately equal amounts of α-eleostearic acid and its isomer, punicic acid, implicating an interactive effect of residues 111 and 115 in punicic acid formation.

Oils rich in conjugated linolenic acids (CLNs)[2] are important medicinally as a source of nutraceuticals and industrially as drying agents in paints, inks, and varnishes (1). CLNs are found as triglycerides in the seed oils of various plant species belonging to the Curcubitaceae, Punicaceae, Bignoniaceae, Rosaceae, Chrysobalanaceae, Lythraceae, Balasaminaceae, and Euphorbiaceae families as either C18 trienes or C18 tetraenes (2, 3). α-Eleostearic acid (α-ESA, 18:3 $\Delta^{9cis,11trans,13trans}$) is the most widespread CLN. Tung (*Aleuites fordii*) and bitter gourd (*Momordica charantia*) seeds are rich source of α-ESA and accumulate >80% and >60% of α-ESA, respectively. Other geometrical isomers of α-ESA that are found in nature are punicic acid (18:3 $\Delta^{9cis,11trans,13cis}$), catalpic acid (18:3 $\Delta^{9trans,11trans,13cis}$), and β-ESA (18:3 $\Delta^{9trans,11trans,13trans}$). Punicic acid is found in pomegranate (*Punica granatum*) and snakegourd (*Trichosanthes kirilowii*) seeds, catalpic acid is present in catalpa (*Catalpa bignonoides* and *Catalpa ovata*) seeds, and β-ESA is present in pomegranate, bitter gourd, and catalpa seeds (4, 5). Additional positional isoforms of α-ESA known are calendic acid (18:3 $\Delta^{8trans,10trans,12cis}$) and jacaric acid (18:3 $\Delta^{8cis,10trans,12cis}$) and are present in pot marigold (*Calendula officinalis*) and jacaranda (*Jacaranda mimosifiola*) seeds, respectively (6, 7).

In recent years cDNAs encoding enzymes that catalyze the formation of conjugated double bonds in CLNs have been identified (8–13). These enzymes were named conjugases (FADXs) and have been shown to be divergent forms of Δ12-oleate desaturases (FAD2). Like FAD2s, FADXs contain histidine motifs that are characteristic of membrane-bound diiron proteins (14). FADXs utilize linoleic acid (18:2 $\Delta^{9cis,12cis}$) and/or linolenic acid (18:3 $\Delta^{9cis,12cis,15cis}$) as a precursor to produce CLNs. Most of the FADXs are bifunctional, possessing both desaturase and conjugase activities (Fig. 1). For example, besides CLNs, Tung FADX can produce the desaturase product, 18:2 $\Delta^{9cis,12trans}$, an isomer of the FAD2-like desaturase product (10). Intriguingly, *Punica* and *Trichosanthes* FADXs can produce a FAD2-like desaturase product, 18:2 $\Delta^{9cis,12cis}$, suggesting that these conjugase enzymes can produce their own substrates (13).

The crystal structures of the soluble desaturases from castor (*Ricinus communis*) and the English Ivy (*Hedera helix*) have given valuable insights into novel catalytic activities and speci-

* This work was supported by the Office of Basic Energy Sciences of the United States Department of Energy (to J. S.) and by National Science Foundation Grant DBI 0701919 (to R. R. and X.-H. Y.). M. S. was supported by the 2010 and 2011 DOE Science Undergraduate Laboratory Internship program.
[S] This article contains supplemental Tables S1–S5.
[1] To whom correspondence should be addressed: Dept. of Biology, Bldg. 463, Brookhaven National Laboratory, 50 Bell Ave., Upton, NY 11973. Tel.: 631-344-3414; Fax: 631-344-3407; E-mail: shanklin@bnl.gov.
[2] The abbreviations used are: CLN, conjugated linolenic acid; aa, amino acids; ESA, eleostearic acid; FAD2, Δ^{12}-oleic acid desaturase; FADX, conjugase; FAME, fatty acid methyl ester.

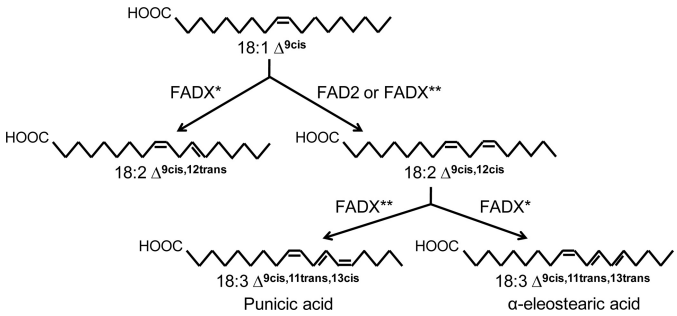

FIGURE 1. **Schematic representation of reactions catalyzed by FAD2 and conjugase enzymes.** * represents tung and *Momordica* FADX; and ** represents *Trichosanthes* or *Punica* FADX.

ficities of the soluble desaturases (15, 16), but the lack of three-dimensional structural information has hampered our understanding of the structure-function relationship of membrane-bound desaturases and FAD2-like divergent enzymes. Structure-function relationships in this class of enzymes have been explored by site-directed mutagenesis, domain swapping, and recently by directed evolution *in vitro* (17–22). Amino acid residues adjacent to the conserved histidine motifs have been shown to contribute to reaction partitioning, and only a handful of amino acid positions have been shown to define substrate specificity (14, 21). For instance, studies on *Arabidopsis* FAD2 and castor fatty acid hydroxylase identified as few as four amino acid positions that exert control over reaction partitioning between hydroxylase and desaturase activity (21, 22).

Evolution of FADXs from FAD2s coupled with the high degree of functional plasticity exhibited by FADXs suggests that identification of key amino acid residues that define their functionality should be feasible. In this context, we sought to identify domains and residues of FADX that are vital for its conjugase activity. Thus, domains of the *Momordica* FADX were swapped with equivalent domains from the *Arabidopsis* FAD2, and the resulting chimeras were heterologously expressed in transgenic *Arabidopsis* seeds. Our results identify two amino acid locations in *Momordica* FADX, 111 and 115, that play key roles in partitioning of catalytic outcome between the formation of α-ESA and its isomer, punicic acid.

EXPERIMENTAL PROCEDURES

Topology Prediction—Prediction of transmembrane helices and topology of *Momordica* conjugase was performed with TMHMM (23), HMMTOP (24), TOP-PRED II (25), and SOSUI (26). The results obtained from these programs were qualitatively similar.

Chimera Construction—Construction of chimeras was carried out using overlap-extension PCR (27). Overlapping fragments of *Arabidopsis* FAD2 and *Momordica* FADX were amplified in separate PCRs using appropriate primer pairs (supplemental Table S1). The PCR products were gel-purified and assembled in a PCR primed with terminal primers and cloned into the pDSRed vector (28) under the control of phaseolin promoter with the use of XmaI and XhoI restriction sites (New England Biolabs). *Momordica* FADX contains 399 amino acids, and *Arabidopsis* FAD2 contains 383 amino acids. Chimera 1 (contains *Momordica* FADX amino acids 1–157; and *Arabidopsis* FAD2 amino acids 149–383), Chimera 2 (FADX aa 1–210; FAD2 aa 202–383), Chimera 3 (FADX aa 1–252; FAD2 aa 244–383), Chimera 4 (FADX aa 1–326; FAD2 aa 317–383), Chimera 5 (FAD2 aa 1–52; FADX aa 61–399), Chimera 6 (FAD2 aa 1–83; FADX aa 93–399), Chimera 7 (FAD2 aa 1–116; FADX aa 126–399), and Chimera 8 (FAD2 aa 1–148; FADX aa 158–399) were constructed in this manner, and the sequence of the chimeras was confirmed by complete nucleotide sequencing.

Site-directed Mutagenesis—Modified FADX genes containing single or multiple mutations were constructed using appropriate templates by overlap-extension PCR as described above. The primers used for site-directed mutagenesis are shown in supplemental Table S1.

Arabidopsis Growth and Transformation—The plants were grown at 22 °C under a 16-h day/8-h night photoperiod. Plants were transformed by employing the floral dip method (29) using the *Agrobacterium tumefaciens* strain GV3101. Individual T1 seeds carrying the transgenes were identified based on DsRed2 expression (30).

Fatty Acid Analysis—Fatty acid methyl esters (FAMES) were prepared from seeds (single or three seeds) by incubation with 30 μl of 0.2 M trimethylsulfonium hydroxide in methanol (31). After drying the samples under a nitrogen stream, the samples were resuspended in hexane. FAMES were analyzed with the use of either a Hewlett-Packard 6890 gas chromatograph-flame ionization detector (Agilent Technologies, Santa Clara, CA) fitted with 60 m $\times$ 250 μm $\times$ 0.25 μm SP-2340 capillary column (Supelco, Bellefonte, PA), or an HP7890A gas chromatograph-mass spectrometer (Hewlett-Packard, Palo Alto, CA) equipped with a HP5975C selective detector (GC/MS) and a 30 m $\times$ 250 μm $\times$ 0.25 μm HP-Innowax capillary column (Agilent Technologies). The injector was maintained at 225 °C, and the oven temperature was varied from 100 to 240 °C at 15 °C/min, then held at 240 °C for 6 min. GC peaks were identified by comparison with authentic standards and by characterization via GC/MS. CLN methyl esters were routinely identified by the presence of an abundant molecular ion at $m/z = 292$ and specific isomers identified by GC retention times compared with an authentic standard mixture of CLN FAMEs. The standard for CLN was obtained from seeds that accumulate different geometrical isomers of C18-conjugated trienoic fatty acids, namely *P. granatum*, *M. charantia* and *C. bignonoides*. *P. granatum* seeds accumulate punicic acid (18:3 $\Delta^{9cis,11trans,13cis}$); *M. charantia* seeds accumulate α-eleostearic acid (18:3 $\Delta^{9cis,11trans,13trans}$); and *C. bignonoides* seeds accumulate catalpic acid (18:3 $\Delta^{9trans,11trans,13cis}$). The percentage values indicating the composition in the fatty acid samples reported are mean values based on at least three individual measurements.

RESULTS

Construction of FADX-FAD2 Chimeras—To identify structural elements that are functionally important in FADX and FAD2, we constructed chimeras comprising domains of *Momordica* FADX fused to those of *Arabidopsis* FAD2. These two enzymes share ~62% sequence identity. To construct chimeras in a rational fashion we first generated a topology model for *Momordica* conjugase based on online computational algo-

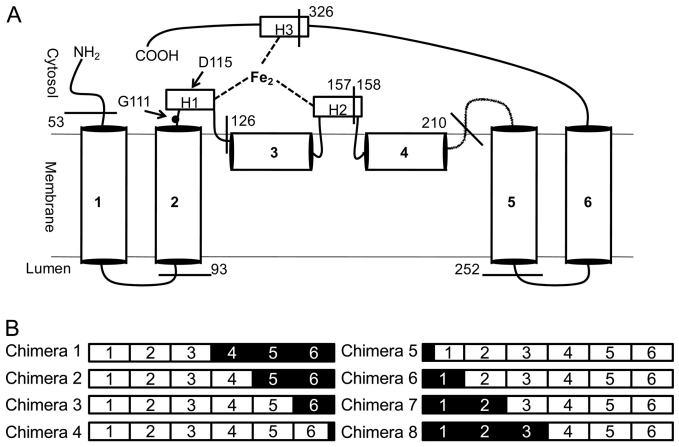

FIGURE 2. **Construction of chimeras.** *A*, proposed topology model for *Momordica* FADX. *H1*, *H2*, and *H3* depict the location of conserved histidine boxes and are shown coordinating to a putative diiron center. Seven cleavage sites where the portions of *Momordica* FADX were replaced with the corresponding *Arabidopsis* FAD2 sequences have been marked on the model. *B*, schematic of chimeric enzyme sequences of *Momordica* FADX and *Arabidopsis* FAD2. Regions in *white boxes* originate from *Momordica* FADX, and regions in *black boxes* from *Arabidopsis* FAD2. For detailed description of the chimeras, see "Experimental Procedures." *C*, amino acid sequence alignment of putative transmembrane helix 2 and first histidine box of *Arabidopsis* FAD2 and *Momordica* FADX. Six residues that differ between the two have been *underlined*.

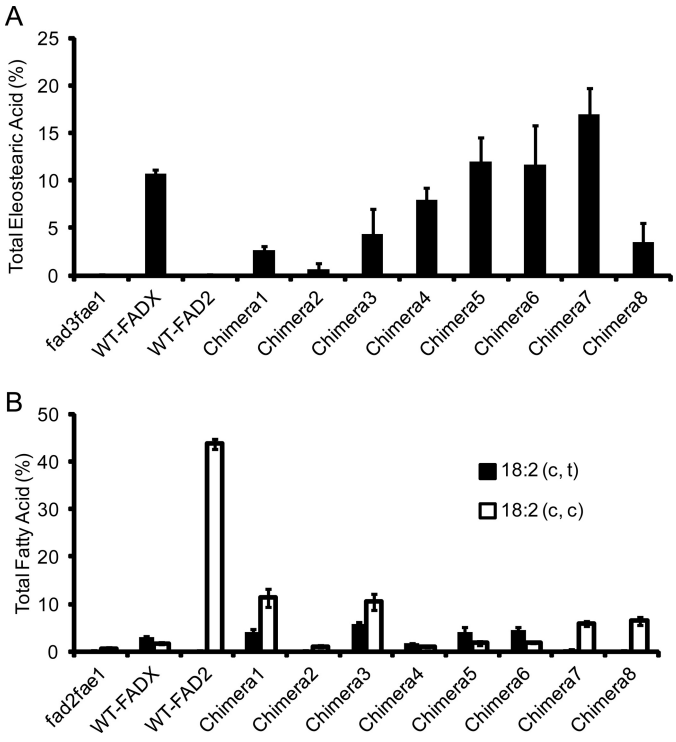

FIGURE 3. **Product accumulation in transgenic *Arabidopsis* seeds expressing wild-type and chimeric enzymes of *Momordica* FADX and *Arabidopsis* FAD2.** *A*, accumulation of total eleostearic acid in transformed *fad3fae1* T1 seeds. *B*, accumulation of desaturation products in transformed *fad2fae1* T1 seeds. Values represent means ± S.D. (*error bars*) of at least three independent analyses.

rithms and previously established topological models (14, 32) (Fig. 2). There are no experimental data available for the topology of either FAD2 or FADX, and the structural models available for other membrane-bound desaturases are derived from their primary structure and *in vivo* activities in yeast (32). Based on the hydropathy plots, the integral membrane fatty acid desaturases and desaturase-like enzymes are predicted to share the same membrane topology (four transmembrane helices and two hairpin domains) and overall three-dimensional structures. Therefore, replacing a particular domain of one of these enzymes with the corresponding domain from the another enzyme is not expected to disrupt the overall structure, and quantification of the fatty acid accumulation would help us to identify domains containing amino acids that control particular properties. To implement this approach seven sites were selected as domain borders that isolate individual helices or hairpin domains within *Momordica* FADX that could be replaced with the corresponding FAD2 sequence as shown in Fig. 2.

Functional Characterization of FADX-FAD2 Chimeras in Arabidopsis fad3fae1—Because the expression of FADX from different origins in yeast results in accumulation of CLNs to <1% (8, 11, 13), we were concerned that potential losses of enzymatic activity resulting from the mapping experiments employing chimeric enzymes would preclude the quantitative product analysis. We therefore chose to express the chimeras and the wild-type (WT) enzymes in *Arabidopsis* under the control of the seed-specific phaseolin promoter (28). To assess conjugase function, these enzymes were transformed into *fad3fae1* double mutant line, which lacks the activity of both the endoplasmic reticulum ω-3 desaturase (FAD3) and the fatty acid elongation 1 (FAE1)-condensing enzyme, and contains elevated level of the FADX substrate, linoleic acid (~52% of the total fatty acids, compared with ~19% in WT) (33).

Previous studies reported *Momordica* FADX-transformed *fad3fae1* seeds accumulate 13% total ESA (34). Consistent with this, FADX-transformed *fad3fae1* T1 seeds in this study showed 9.9% of total ESA accumulation with an isomer distribution of 7.7% α-ESA, 0.2% punicic acid, and 2.1% β-ESA. Chimeras 1–4 and 8 produced lower total ESA (<7.5%) compared with WT-FADX. Chimeras 5 and 6 accumulated ~11% total ESA, whereas Chimera 7 accumulated ~17% total ESA (Fig. 3*A* and supplemental Table S2). Intriguingly, Chimera 7 displayed a different product distribution of CLN isomers relative to that of WT-FADX in accumulating 8.9% of punicic acid in addition to 7.8% α-ESA (Figs. 4 and 5*A*). In the absence of protein quantitation data we are unable to determine whether changes in ESA accumulation result from changes in enzyme activity or changes in enzyme levels.

Functional Characterization of FADX-FAD2 Chimeras in fad2fae1—To test the presence of FAD2-like desaturase functionality, the individual chimeras and the WT enzymes were transformed into the *Arabidopsis fad2fae1* background as these lines contain ~86% of the FAD2 substrate 18:1Δ^{9cis} and <1% of 18:2. Additionally, because *fad2fae1* seeds contain only ~0.6% of 18:2 $\Delta^{9cis,12cis}$, the accumulation of any ESA above this level must result from FAD2-like desaturase activity of the introduced enzyme. Analysis of the transformed *fad2fae1* seeds showed that the *Arabidopsis* WT-FAD2 produced ~43.7% of

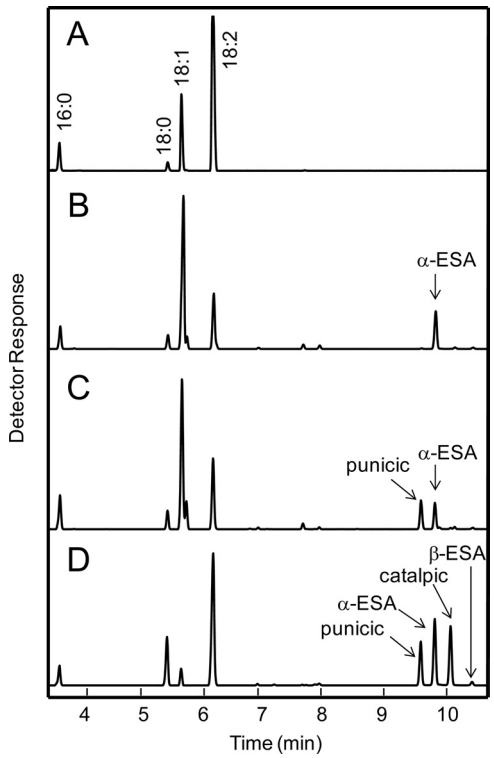

FIGURE 4. **GC analyses of FAMEs extracted from transgenic *Arabidopsis* seeds.** *A*, untransformed *fad3/fae1*. *B* and *C*, transformed with wild-type *Momordica* FADX (*B*) and Chimera 7 (*C*). *D*, standard of FAMEs from seeds that accumulate different isomers of C18-conjugated trienoic fatty acids. Standard includes FAMEs from seeds of *P. granatum*, *M. charantia*, and Southern Catalpa which accumulate punicic acid, α-ESA, and catalpic acid, respectively.

18:2 $\Delta^{9cis,12cis}$ (Fig. 3*B* and supplemental Table S3). As reported previously, WT-FADX showed diverse functionality (35). Besides ~1.6% total ESA and ~3% of 18:2 $\Delta^{9cis,12trans}$, the WT-FADX-transformed seeds accumulated 1.7% of 18:2 $\Delta^{9cis,12cis}$. Although the accumulation of total ESA in *fad2fae1* (<0.8%) was much lower than in *fad3fae1*, high levels of 18:2 $\Delta^{9cis,12cis}$ (>6.5%) accumulated upon expression of Chimeras 1, 3, and 8 (Fig. 3 and supplemental Table S3). Expression of Chimeras 2 and 4 resulted in no detectable amount of ESA and ~1% of 18:2 $\Delta^{9cis,12cis}$ in the transformed seeds. Chimeras 5 and 6 produced ~2.0% of total ESA and ~2.0% of 18:2 $\Delta^{9cis,12cis}$. Expression of Chimera 7 in *fad2fae1* seeds resulted in the accumulation of ~7.9% ESA, and the average level of punicic acid and α-ESA in Chimera 7 transformants was 4.6 and 3.1%, respectively (Fig. 5*B*). Chimera 7 also produced 6.2% of 18:2 $\Delta^{9cis,12cis}$ (Fig. 3 and supplemental Table S3) in addition to ~0.5% of 18:2 $\Delta^{9cis,12trans}$ isomer. Furthermore, Chimera 6 produced higher levels of 18:2 $\Delta^{9cis,12trans}$ whereas Chimera 7 produced more of the 18:2 $\Delta^{9cis,12cis}$ isomer (Fig. 3*B*).

Six Amino Acids Located in Transmembrane Helix 2 Play Important Role in Determining Desaturase and Conjugase Functionalities—Chimeras 6 and 7 are fusions between the N terminus of FAD2 and the C terminus of FADX, the difference being that Chimera 7 contains the first two helices and first portion of the tripartite conserved histidine motif 1 (13) of FAD2, whereas Chimera 6 only contains the first helix of FAD2, the balance of the protein consists of FADX. That Chimera7 produced a mixture of α-ESA and punicic acid, whereas Chimera 6 produced primarily α-ESA (like *Momordica*) suggests that both the ability to produce punicic acid and the increase in total ESA accumulation must be specified by the six amino acid differences between FAD2 and FADX in helix 2 and first histidine box (Fig. 2). To test this hypothesis, the $FADX_6$mut was engineered consisting of V97L, F100A, A104C, M109I, G111V, and D115E (using *Momordica* FADX numbering), in which the six WT-FADX residues were replaced by the corresponding residues from WT-FAD2.

Analysis of the transformed seeds confirmed that the $FADX_6$mut was functionally similar to Chimera 7 in producing 20.1% total ESA in *fad3fae1* lines (Fig. 5*A* and supplemental Table S4); and 7.8% total ESA in *fad2fae1* lines (Fig. 5*B* and supplemental Table S5). Further, the $FADX_6$mut like Chimera 7 produces both punicic and α-ESA (9.5% punicic acid and 9.5% α-ESA in *fad3fae1* lines, and 4.1% punicic acid and 3.3% α-ESA in *fad2fae1* lines). Expression of the $FADX_6$mut in *fad2fae1 Arabidopsis* background shows that it also produces 7.1% of 18:2 $\Delta^{9cis,12cis}$, *i.e.* it has a desaturase activity that is responsible for the production of substrate for its own conjugase activity.

Substitutions of G111V and D115E in Momordica FADX Are Sufficient for Significant Punicic Acid Accumulation—To determine whether any single amino acid of the six substitutions in $FADX_6$mut has a major impact on product partitioning between α-ESA and punicic acid, we constructed a series of six drop-out $FADX_5$mut genes in which each of the six amino acid substituents was individually converted back to its FADX equivalent. The constructs were transformed into both *fad3fae1* and *fad2fae1 Arabidopis* backgrounds. Analysis of the transformed seeds showed that four of the six dropout mutants, *i.e.* $FADX_6$mut-V97L (contains all of the six FAD2 substitutions except V97L), $FADX_6$mut-F100A, $FADX_6$mut-A104C, and $FADX_6$mut-M109I had conjugase activities similar to that of the $FADX_6$mut (Figs. 5 and 6), indicating that substitutions at positions 97, 100, 104, and 109 do not contribute to the increase in ESA accumulation or the product distribution of $FADX_6$mut enzyme.

In contrast, $FADX_6$mut-G111V resulted in much lower ESA accumulation relative to the $FADX_6$mut and eliminated the accumulation of punicic acid (Fig. 5 and supplemental Tables S4 and S5), suggesting a key role of residue 111 in imparting *Trichosanthes*-like (punicic acid-producing) conjugase activity to $FADX_6$mut. Supporting this observation, the single mutant FADX G111V produced 20.4% ESA in *fad3fae1*- and 11.6% ESA in *fad2fael*-transformed seeds. However, G111V accumulated higher α-ESA compared with $FADX_6$mut (16.1% *versus* 9.5% in *fad3fae1*, and 8.4% *versus* 3.3% in *fad2fae1*), but considerably lower amounts of punicic acid compared with the $FADX_6$mut (2.8% *versus* 9.5% in *fad3fae1*, and 2.2% *versus* 4.1% in *fad2fae1*). Furthermore, it is interesting to note that the single mutant G111V produced 5.6% of 18:2 $\Delta^{9cis,12cis}$ (Fig. 6 and supplemental Table S5), suggesting that Val at position 111 near the active site is important for imparting FAD2-like desaturase functionality.

Although $FADX_6$mut-D115E showed a modest reduction of ESA accumulation relative to the $FADX_6$mut (15.0% *versus* 20.1%, supplemental Table S4), punicic acid accumulation was decreased by ~75% compared with $FADX_6$mut (2.1% *versus*

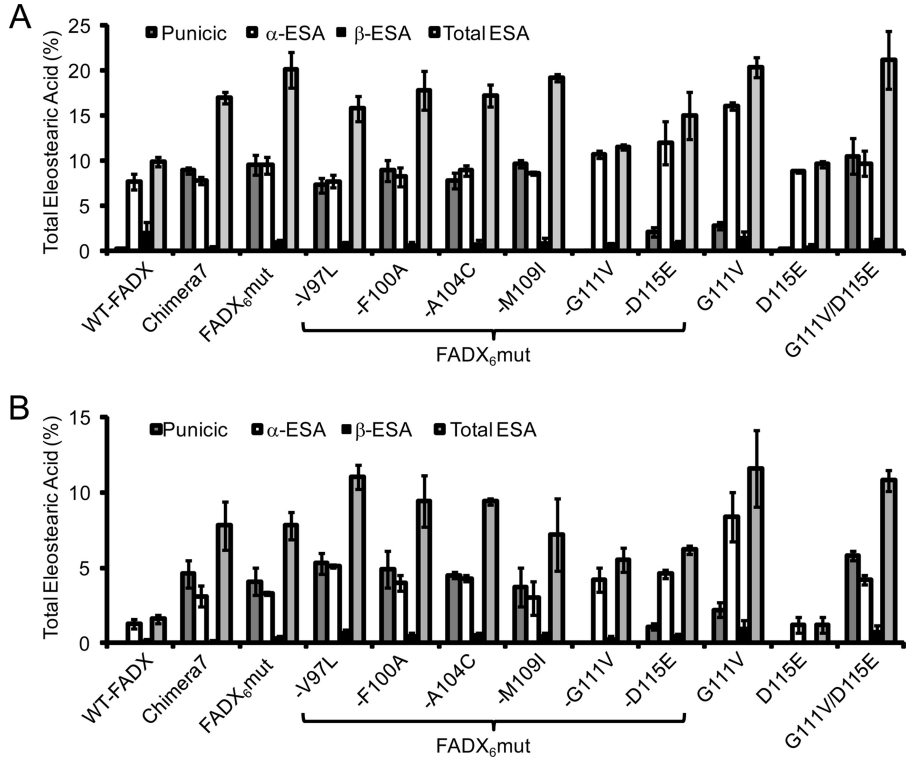

FIGURE 5. **Levels of ESA accumulated in wild-type or mutant *Momordica* FADX transformed *fad3fae1* (*A*) and *fad2fae1* (*B*) seeds.** To test the contribution of individual amino acid substitutions to the activity of $FADX_6$mut gene, each of the six amino acid was individually substituted for its FAD2 equivalent to create six modified FADX genes. For example, enzyme $FADX_6$mut-V97L contains five substitutions F100A, A104C, M109I, G111V, and D115E, and so on. Values represent means ± S.D. (*error bars*) of at least three independent analyses.

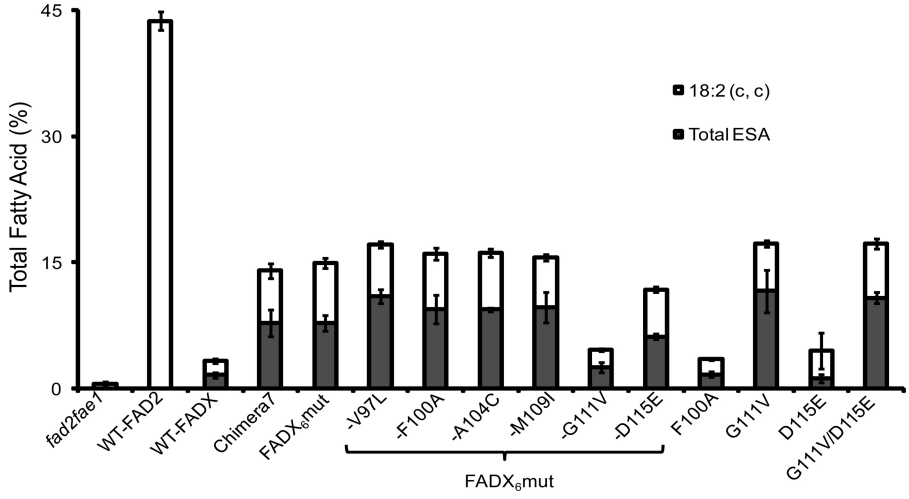

FIGURE 6. **Levels of 18:2 (c, c) product and total eleostearic acid accumulating in *Arabidopsis fad2fae1* seeds upon the expression of wild-type *Arabidopsis* FAD2, wild-type *Momordica* FADX, or mutant *Momordica* FADX constructs as described in Fig. 5 legend.** Values represent means ± S.D. (*error bars*) of at least three independent analyses.

9.5% in *fad3fae1*, and 1.1% *versus* 4.1% in *fad2fae1*, supplemental Tables S4 and S5). This result suggests that position 115 also plays a role in imparting *Trichosanthes*-like conjugase activity to WT-FADX. However, the single mutant D115E displayed activity like WT-FADX, with respect to total ESA and punicic acid accumulation. This implies that D115E alone cannot enhance ESA accumulation.

We therefore investigated the possibility that D115E and G111V substitutions in combination are responsible for additional ESA accumulation by analyzing the expression of a FADX G111V/D115E double mutant. Analysis of the transformed seeds show that the conjugase double mutant produced 21.2% of total ESA compared with 9.9% for WT-FADX in *fad3fae1* and 10.8% *versus* 1.6% in *fad2fae1*, respectively (supplemental Tables S4 and S5). Besides increased α-ESA, the double mutant resulted in significant punicic acid accumulation (10.5% punicic acid and 9.7% α-ESA in *fad3fae1*; and 5.8% punicic acid and 4.2% α-ESA in *fad2fae1*, Fig. 5). This result suggests that just two amino acid changes, G111V/D115E, are sufficient to impart significant *Trichosanthes*-like conjugase

functionality to the *Momordica* conjugase. Further, the double mutant had increased FAD2-like functionality and produced 6.4% of 18:2 $\Delta^{9cis,12cis}$ compared with 1.7% for WT-FADX (Fig. 6 and supplemental Table S5).

DISCUSSION

Through our approach of analyzing the products of *Momordica* FADX-*Arabidopsis* FAD2 chimeric enzymes by expression in various *Arabidopsis* mutant backgrounds we identified Chimera 7, which accumulated higher ESA relative to WT-FADX. In this analysis our interpretation is restricted to accumulation of total ESA in transformed seeds because no determination of differential fatty acid turnover was made. Further analysis revealed that the increase of ESA upon expression of Chimera 7 was associated with substantially elevated punicic acid production and equivalent levels of α-ESA production relative to WT-FADX. Subsequent targeted mutagenesis identified residues 111 and 115 as the two key residues that influence both ESA accumulation and reaction partitioning. Expression of FADX G111V in *fad3fae1*-transformed seeds resulted in a 14-fold increase in punicic acid and 2-fold increase in α-ESA accumulation relative to WT-FADX. Although FADX D115E showed similar ESA accumulation as WT-FADX, the double mutant FADX G111V/D115E led to a 50-fold increase in punicic acid accumulation in the same background. This result implies that the difference with respect to partitioning of conjugase product into its geometrical isomers is directly determined by the identity of the amino acid residues at positions 111 and 115. Further, the bulkier residues in the G111V/D115E double mutant appear to interact because we observed an increase in punicic acid formation but no change in total ESA accumulation (relative to G111V). We further tested the substitution of Gly at position 111 with a range of side chains of different bulk; *i.e.* the larger Leu and Phe, and the smaller Ala compared with Val. We made each of these mutations with Asp or Glu at position 115. Although these changes had little effect on product partitioning, each of these substitutions resulted in a decrease in ESA accumulation relative to G111V and G111V/D115E (supplemental Tables S4 and S5), suggesting that Val has an optimal side chain bulk at position 111.

Conjugases from *Trichosanthes* and *Punica* accumulate punicic acid in WT-*Arabidopsis* seeds when heterologously expressed under the control of napin promoter (13). The average amounts of punicic acid in *Trichosanthes* and *Punica* conjugase transformants have been reported to be 3.5% and 2.3%, respectively, with maximal amounts reaching 10.2% and 4.4%, respectively. Interestingly, in transformed *fad3fae1 Arabidopsis* seeds, besides 9.7% of α-ESA, the expression of FADX G111V/D115E results in the accumulation of an additional 10.5% of punicic acid. According to the predicted structural model (Fig. 2), residues 111 and 115 are located in or adjacent to the first of the three conserved histidine boxes. Specifically, position 115 immediately follows the first histidine residue of the histidine cluster, and residue 111 would therefore be positioned one helical turn before residue 115, suggesting that these side chains are adjacent to one another and bracket a conserved histidine within the active site. It is interesting to note that the other four residues in helix 2 that differ between FAD2 and FADX which do not influence functionality are not predicted to occur near the active site histidine cluster. The absence of a crystal structure for any membrane-bound desaturase represents a major impediment to understanding of the mechanisms underlying these results.

Various chemical mechanisms have been proposed to describe the biological origin of conjugated trienoic acids. It has been shown that during conversion of linoleic acid to calendic acid in *C. officinalis* developing seeds, hydrogen is abstracted sequentially from the C8 and C11 methylene groups that flank the cis-Δ9 double bond of linoleic acid, a mechanism known as "1,4-desaturation" (36, 37). The production of α-ESA is proposed to involve the removal of hydrogens from the C11 and C14 methylene groups that flank the cis-Δ12 double bond of linoleic acids (34). In contrast, little mechanistic information is presently known about the formation of geometrical isomers of ESA such as punicic acid and α-ESA.

In previous work on the evolutionarily distinct acyl-ACP desaturases, for which the geometry of the substrate binding cavity is defined from crystal structures, the production of allylic hydroxy fatty acids was rationalized by a relative shift of the fatty acid substrate with respect to the active site Fe-O oxidant. The boomerang shape of the substrate binding cavity imposes an eclipsed conformation on the acyl chain that causes the pro-*R* hydrogens to be presented to the active site oxidant bound to the diiron active site (15, 16). Although the amino acid sequences of acyl-ACP desaturases and integral membrane FAD2 desaturases differ, the common chemical imperative imposed by the stereochemistry of desaturation implies that the shapes of the substrate binding cavities relative to the active site iron oxidant species will be similar.

Based on the data presented here, and by analogy to mechanisms proposed for the acyl-ACP desaturases (38) involving shifting the register of the bound fatty acid substrate relative to the active site, the formation of either punicic acid or α-ESA can perhaps be rationalized in terms of distinct proposed substrate binding modes relative to the position of the oxidant and the envisaged bend in the substrate binding cavity. It is likely that punicic acid results from the placement of C12 and C13 of the 18:2 $\Delta^{9cis,12cis}$ substrate at the bend in the binding cavity wherein the bulkier residues constrain the product in a *cis* configuration at C13, whereas α-ESA is produced when the substrate 18:2 $\Delta^{9cis,12cis}$ binds deeper into the binding cavity wherein the smaller residues allow the product to adopt a more stable anti-conformation that results in pro-S hydrogen removal at C14 and thence trans-double bond formation. In the case of the single mutant, G111V, steric bulk presented by a larger Val residue causes the substrate to bind two carbons less deeply in the active site leading to conversion of 18:2 $\Delta^{9cis,12cis}$ to punicic acid, and in the case of the double mutant, G111V/D115E, conversion of 18:2 $\Delta^{9cis,12cis}$ to punicic acid is much enhanced due to larger steric bulk presented by the presence of larger residues Val and Glu near the active site.

Position 111 was also found to be crucial for imparting FAD2-like desaturase functionality to *Momordica* conjugase (Fig. 6). In *fad2fae1* lines, the single mutant G111V produced 3-fold more 18:2 $\Delta^{9cis,12cis}$ and 8-fold more ESA compared with WT-FADX. Perhaps this higher FAD2-like desaturase function

```
McFADX      LAWPVYWFCQGAVLTGMWGIAHDCGHH
CiFADX      LAWLLYWAVQGCFFTGAWALAHDCGHH
LmFADX      LAWLLYWAVQGCFFTGAWALAHDCGHH
IbFADX      VAWPIYWAIQGCVQLGILVLGHECGHH
VfFADX      IAWPVYWAFQGCILTSVWVLGHECGHH
TkFADX      LAWPLYWFCQGSVFTGLWVIAHECGHR
PgFADX      MAWPVYWFLQGSNMLGIWVIAHECGHQ
RcFAH       VAWLVYWLFQGCILTGLWVIGHECGHH
LfFAH       LAWPLYWVCQGCVLTGIWVIGHECGHH
CpFAH       VLWSIYTVLQGLFATGLWVIGHECGHC
CaAcetyl    LAWPLYWFCQASILTGLWVIGHECGHH
CpalEpoxy   LAWPVYWFCQASVLTGLWILGHECGHH
VfFAD2      VAWPIYWALQGCVLTGVWVIAHECGHH
TkFAD2      IAWPLYWIFQGCSLTGVWVIAHECGHH
PgFAD2      AAWPVYWALQGCVLTGVWVIAHECGHH
AtFAD2      LAWPLYWACQGCVLTGIWVIAHECGHH
              * :*   *.    .   :.*:***
```

FIGURE 7. **Amino acid sequence alignment of the amino acids comprising putative transmembrane helix 2 and the first histidine box from various classes of FAD2 and FAD2-like enzymes.** Each enzyme modifies the Δ^{12} position of fatty acid substrates. Sequence sources and their accession numbers: conjugase from *M. charantia* (McFADX), AF182521; conjugase from coco plum (*C. icaco;* CiFADX), BD224609.1; conjugase from gopher apple (*Licania michauxii*; LmFADX) BD224612.1; conjugase from *Impatiens balsamina* (IbFADX), AF182520; conjugase from tung (*Vernicia fordii*; VfFADX) AF525535; conjugase from *T. kirilowii* (TkFADX) AY178444; conjugase from *P. granatum* (PgFADX) AY178446; hydroxylase from castor (*R. communis;* RcFAH) EU523112; hydroxylase from *Lesquerella fendleri* (LfFAH) AF016103; hydroxylase from *Claviceps purpurea* (EU661785); acetylenase from *C. alpina* (CaAcetyl) Y16285; epoxygenase from *Crepis palaestina* (CpalEpoxy) Y16283; FAD2 from tung (VfFAD2) AF525534; FAD2 from *T. kirilowii* (TkFAD2) AY178445; FAD2 from *P. granatum* (PgFAD2) AY178447; FAD2 from *Arabidopsis thaliana* (AtFAD2) L26296.

attributable to the G111V mutation allows the enzyme to perform the two consecutive reactions to produce ESA from 18:1 without release of the product of the desaturation reaction. Such a mechanism could help explain higher ESA accumulation in seeds transformed with G111V. As described above, perhaps we can rationalize the formation of 18:2 $\Delta^{9cis,12cis}$ and 18:2 $\Delta^{9cis,12trans}$ in terms of distinct binding modes of the 18:1Δ^{9cis} substrate relative to the position of the active site oxidant and the bend in the active-site cavity. In the case of less steric hindrance in the active site the more stable product 18:2$\Delta^{9cis,12trans}$ can form.

In other FAD2-related work, subtle changes near the active site have been shown to play a key role in influencing desaturation and hydroxylation product partitioning (21, 22). We therefore performed alignments of the amino acid sequences of helix 2 and the first histidine box of various FAD2s and FAD2-like enzymes that modify the C12 position of fatty acids (Fig. 7). Our sequence analysis shows that position 111 is mostly conserved as a hydrophobic residue Val in FAD2s and FAD2-like enzymes. It is replaced by a smaller hydrophobic residue Gly in *Momordica*; and by Ala in coco plum (*Chrysobalanus icaco*) and gopher apple (*Licania michauxii*) conjugases. Coco plum and gopher apple conjugases are closely related and have shown to accumulate α-ESA in soybean somatic embryos (39). The epoxygenase contains an Ile at this position. Position 115 is mostly conserved as Glu in FAD2s and FAD2-like enzyme. It is replaced by a smaller residue Asp in *Momordica*, coco plum, and gopher apple conjugases. Notably, most of the FAD2 desaturase-like variant enzymes that are bifunctional and possess residual FAD2-like desaturase activity (*Trichosanthes* conjugase, *Punica* conjugase, *Lesquerella* hydroxylase, castor hydroxylase, *Claviceps* hydroxylase, *Crepis* acetylenase) contain Val and Glu at positions 111 and 115, respectively (Fig. 7). Although the identities of amino acids at positions 111 and 115 are conserved as Val and Glu in tung conjugase and *Crepis alpina* acetylenase, tung conjugase has been shown to produce 18:2 $\Delta^{9cis,12trans}$, and not 18:2 $\Delta^{9cis,12cis}$, the FAD2-like desaturase product; and *C. alpina* acetylenase preferentially produces 18:2 $\Delta^{9cis,12trans}$ (10, 40, 41). This suggests that in the case of tung conjugase and *C. alpina* acetylenase some additional changes near the active site may be necessary for introducing preferential FAD2-like desaturase activity.

In summary, the data presented here support the view that a small number of residues at key positions in the vicinity of the active site can have a profound impact on catalytic outcome of the membrane-bound desaturase-like enzymes. These studies identified *Momordica* conjugase mutants, G111V and G111V/D115E, which provide an increased understanding of the specificity determinants of fatty acid conjugases; in addition, their expression results in the accumulation of substantially elevated levels of ESA in *Arabidopsis* seeds relative to the WT-FADX conjugase. Such variants may have utility for the accumulation of industrially relevant levels of ESA in crop plants.

Acknowledgment—We thank Dr. Edgar B. Cahoon (University of Nebraska-Lincoln) for providing Momordica FADX DNA.

REFERENCES

1. Biermann, U., Bornscheuer, U., Meier, M. A., Metzger, J. O., and Schäfer, H. J. (2011) Oils and fats as renewable raw materials in chemistry. *Angew Chem. Int. Ed. Engl.* **50,** 3854–3871
2. Smith, C. R., Jr. (1971) Occurrence of unusual fatty acids in plants. *Prog. Chem. Fats Other Lipids* **11,** 137–177
3. Badami, R. C., and Patil, K. B. (1980) Structure and occurrence of unusual fatty acids in minor seed oils. *Prog. Lipid Res.* **19,** 119–153
4. Ozgul-Yucel, S. (2005) Determination of conjugated linolenic acid content of selected oil seeds grown in Turkey. *J. Am. Oil Chem. Soc.* **82,** 893–897
5. Joh, Y. G., Kim, S. J., and Christie, W. W. (1995) The structure of the triacylglycerols, containing punicic acid, in the seel oil of *Trichosanthes kirilowii*. *J. Am. Oil Chem. Soc.* **72,** 1037–1042
6. McClean, J., and Clark, A. H. (1956) Isolation of octadec-8,10,12-trienoic acid from marigold seed oil. *J. Chem. Soc.* **1956,** 777–778
7. Hopkins, C. Y., and Chisholm, M. J. (1968) A survey of the conjugated fatty acids of seed oils. *J. Am. Oil Chem. Soc.* **45,** 176–182
8. Cahoon, E. B., Carlson, T. J., Ripp, K. G., Schweiger, B. J., Cook, G. A., Hall, S. E., and Kinney, A. J. (1999) Biosynthetic origin of conjugated double bonds: production of fatty acid components of high-value drying oils in transgenic soybean embryos. *Proc. Natl. Acad. Sci. U.S.A.* **96,** 12935–12940
9. Cahoon, E. B., Ripp, K. G., Hall, S. E., and Kinney, A. J. (2001) Formation of conjugated Δ8,Δ10-double bonds by Δ12-oleic-acid desaturase-related enzymes: biosynthetic origin of calendic acid. *J. Biol. Chem.* **276,** 2637–2643
10. Dyer, J. M., Chapital, D. C., Kuan, J. C., Mullen, R. T., Turner, C., McKeon, T. A., and Pepperman, A. B. (2002) Molecular analysis of a bifunctional fatty acid conjugase/desaturase from tung: implications for the evolution of plant fatty acid diversity. *Plant Physiol.* **130,** 2027–2038
11. Qiu, X., Reed, D. W., Hong, H., MacKenzie, S. L., and Covello, P. S. (2001)

Identification and analysis of a gene from *Calendula officinalis* encoding a fatty acid conjugase. *Plant Physiol.* **125,** 847–855
12. Hornung, E., Pernstich, C., and Feussner, I. (2002) Formation of conjugated Δ11Δ13-double bonds by Δ12-linoleic acid (1,4)-acyl-lipid-desaturase in pomegranate seeds. *Eur. J. Biochem.* **269,** 4852–4859
13. Iwabuchi, M., Kohno-Murase, J., and Imamura, J. (2003) Δ12-oleate desaturase-related enzymes associated with formation of conjugated trans-Δ11,cis-Δ13 double bonds. *J. Biol. Chem.* **278,** 4603–4610
14. Shanklin, J., Whittle, E., and Fox, B. G. (1994) Eight histidine residues are catalytically essential in a membrane-associated iron enzyme, stearoyl-CoA desaturase, and are conserved in alkane hydroxylase and xylene monooxygenase. *Biochemistry* **33,** 12787–12794
15. Lindqvist, Y., Huang, W., Schneider, G., and Shanklin, J. (1996) Crystal structure of Δ9 stearoyl-acyl carrier protein desaturase from castor seed and its relationship to other di-iron proteins. *EMBO J.* **15,** 4081–4092
16. Guy, J. E., Whittle, E., Kumaran, D., Lindqvist, Y., and Shanklin, J. (2007) The crystal structure of the ivy Δ4–16:0-ACP desaturase reveals structural details of the oxidized active site and potential determinants of regioselectivity. *J. Biol. Chem.* **282,** 19863–19871
17. Libisch, B., Michaelson, L. V., Lewis, M. J., Shewry, P. R., and Napier, J. A. (2000) Chimeras of Δ6-fatty acid and Δ8-sphingolipid desaturases. *Biochem. Biophys. Res. Commun.* **279,** 779–785
18. Sayanova, O., Beaudoin, F., Libisch, B., Shewry, P., and Napier, J. (2000) Mutagenesis of the borage Δ(6) fatty acid desaturase. *Biochem. Soc. Trans.* **28,** 636–638
19. Meesapyodsuk, D., Reed, D. W., Covello, P. S., and Qiu, X. (2007) Primary structure, regioselectivity, and evolution of the membrane-bound fatty acid desaturases of *Claviceps purpurea*. *J. Biol. Chem.* **282,** 20191–20199
20. Vanhercke, T., Shrestha, P., Green, A. G., and Singh, S. P. (2011) Mechanistic and structural insights into the regioselectivity of an acyl-CoA fatty acid desaturase via directed molecular evolution. *J. Biol. Chem.* **286,** 12860–12869
21. Broun, P., Shanklin, J., Whittle, E., and Somerville, C. (1998) Catalytic plasticity of fatty acid modification enzymes underlying chemical diversity of plant lipids. *Science* **282,** 1315–1317
22. Broadwater, J. A., Whittle, E., and Shanklin, J. (2002) Desaturation and hydroxylation: residues 148 and 324 of *Arabidopsis* FAD2, in addition to substrate chain length, exert a major influence in partitioning of catalytic specificity. *J. Biol. Chem.* **277,** 15613–15620
23. Krogh, A., Larsson, B., von Heijne, G., and Sonnhammer, E. L. (2001) Predicting transmembrane protein topology with a hidden Markov model: application to complete genomes. *J. Mol. Biol.* **305,** 567–580
24. Tusnády, G. E., and Simon, I. (1998) Principles governing amino acid composition of integral membrane proteins: application to topology prediction. *J. Mol. Biol.* **283,** 489–506
25. Claros, M. G., and von Heijne, G. (1994) TopPred II: an improved software for membrane protein structure predictions. *Comput. Appl. Biosci.* **10,** 685–686
26. Mitaku, S., Ono, M., Hirokawa, T., Boon-Chieng, S., and Sonoyama, M. (1999) Proportion of membrane proteins in proteomes of 15 single-cell organisms analyzed by the SOSUI prediction system. *Biophys. Chem.* **82,** 165–171
27. Horton, R. M., Cai, Z. L., Ho, S. N., and Pease, L. R. (1990) Gene splicing by overlap extension: tailor-made genes using the polymerase chain reaction. *BioTechniques* **8,** 528–535
28. Pidkowich, M. S., Nguyen, H. T., Heilmann, I., Ischebeck, T., and Shanklin, J. (2007) Modulating seed β-ketoacyl-acyl carrier protein synthase II level converts the composition of a temperate seed oil to that of a palm-like tropical oil. *Proc. Natl. Acad. Sci. U.S.A.* **104,** 4742–4747
29. Clough, S. J., and Bent, A. F. (1998) Floral dip: a simplified method for *Agrobacterium*-mediated transformation of *Arabidopsis thaliana*. *Plant J.* **16,** 735–743
30. Stuitje, A. R., Verbree, E. C., van der Linden, K. H., Mietkiewska, E. M., Nap, J. P., and Kneppers, T. J. (2003) Seed-expressed fluorescent proteins as versatile tools for easy (co)transformation and high-throughput functional genomics in *Arabidopsis*. *Plant Biotechnol. J.* **1,** 301–309
31. Butte, W., Eilers, J., and Hirsch, K. (1982) Trialkylsulfonium-hydroxides and trialkylselonium-hydroxides for the pyrrolytic alkylation of acidic compounds. *Anal. Lett.* **15,** 841–850
32. van Beilen, J. B., Penninga, D., and Witholt, B. (1992) Topology of the membrane-bound alkane hydroxylase of *Pseudomonas oleovorans*. *J. Biol. Chem.* **267,** 9194–9201
33. Smith, M. A., Moon, H., Chowrira, G., and Kunst, L. (2003) Heterologous expression of a fatty acid hydroxylase gene in developing seeds of *Arabidopsis thaliana*. *Planta* **217,** 507–516
34. Cahoon, E. B., Dietrich, C. R., Meyer, K., Damude, H. G., Dyer, J. M., and Kinney, A. J. (2006) Conjugated fatty acids accumulate to high levels in phospholipids of metabolically engineered soybean and *Arabidopsis* seeds. *Phytochemistry* **67,** 1166–1176
35. Yang, P., Li, X., Shipp, M. J., Shockey, J. M., and Cahoon, E. B. (2010) Mining the bitter melon (*Momordica charantia* L.) seed transcriptome by 454 analysis of non-normalized and normalized cDNA populations for conjugated fatty acid metabolism-related genes. *BMC Plant Biol.* **10,** 250
36. Crombie, L., and Holloway, S. J. (1985) The biosynthesis of calendic acid, octadeca-(8*E*,10*E*,12*Z*)-trienoic acid, by developing marigold seeds: origins of (*E*,*E*,*Z*) and (*Z*,*E*,*Z*) conjugated triene acids in higher plants. *J. Chem. Soc. Perkin Trans.* 2425–2434
37. Reed, D. W., Savile, C. K., Qiu, X., Buist, P. H., and Covello, P. S. (2002) Mechanism of 1,4-dehydrogenation catalyzed by a fatty acid (1,4)-desaturase of *Calendula officinalis*. *Eur. J. Biochem.* **269,** 5024–5029
38. Whittle, E. J., Tremblay, A. E., Buist, P. H., and Shanklin, J. (2008) Revealing the catalytic potential of an acyl-ACP desaturase: tandem selective oxidation of saturated fatty acids. *Proc. Natl. Acad. Sci. U.S.A.* **105,** 14738–14743
39. Cahoon, E. B., Carlson, T. J., Hitz, W. D., and Ripp, K. G. (July 17, 2007) U.S. Patent 7,244,563
40. Gagné, S. J., Reed, D. W., Gray, G. R., and Covello, P. S. (2009) Structural control of chemoselectivity, stereoselectivity, and substrate specificity in membrane-bound fatty acid acetylenases and desaturases. *Biochemistry* **48,** 12298–12304
41. Carlsson, A. S., Thomaeus, S., Hamberg, M., and Stymne, S. (2004) Properties of two multifunctional plant fatty acid acetylenase/desaturase enzymes. *Eur. J. Biochem.* **271,** 2991–2997